scientific reports

Check for updates

OPEN

Optimization analysis of air cooled open cathode proton exchange membrane fuel cell flow channel structure

Zhijun Deng[1], Qingwei Wang[2], Xun Fang[2], Yaru Han[1], Kunxiang Liu[2]✉ & Chen Zhao[2]✉

The cathode channel of air-cooled open-cathode proton exchange membrane fuel cell (AO-PEMFC) is both a reactant supply channel and a cooling and heat dissipation channel, and its structural design is a key factor affecting its output performance. Firstly, the numerical study of AO-PEMFC with different cathode channel bending angles was carried out, and the results showed that the output performance of a single cell with a cathode bending angle of 2.5° was improved by 3.88% compared with that of a single cell with a cathode straight channel at rated point-density electricity, and the cathode voltage drop increased by only 1.5%. In addition, in order to further improve the power density of the fuel cell, two agent models, support vector regression and Gaussian process regression, are constructed and trained, and a genetic algorithm is used to find the parameter optimization for the bending angle, width and height of the cathode channel. Finally, the proposed ranges of width, height and bending angle of the optimal flow channel are obtained, which are w = 1.1–1.2 mm, d = 1.3–1.5 mm and θ = 2.23°–2.99°, respectively, and the output power density of a single cell within this range will be no less than 0.489 W/cm^2.

Keywords Air-cooled open-cathode proton exchange membrane fuel cell, Structure optimization, Genetic algorithm, Power density

Fuel cell is the core direction of efficient utilization of hydrogen energy, and AO-PEMFC is even more compact, lightweight, environmentally friendly, efficient, low operating temperature, etc., which has a broad application prospect in various scenarios such as power supply for unmanned aerial vehicles and mobile power generation equipment[1–4]. However, it still faces many problems in its commercialization phase. For example, it is important to quickly predict the response of cell output performance after changes in cell boundaries (meaning operating conditions, membrane electrode physical property parameters, polar plate structure parameters, etc.). With the continuous development of the machine learning field in recent years, it has become a new research hotspot to take a data-driven approach to the parameter optimization study of fuel cells[5–8]. Therefore, the prediction and optimization of target parameters such as cell power density under different boundary conditions through numerical simulation combined with artificial intelligence methods can save a large number of experiments and give the suggested values of cell parameters for obtaining optimal output performance faster without loss of accuracy[9–11].

There have been many studies on the optimization of proton exchange membrane fuel cell parameters. Mohamed et al.[12] optimized the number of single cells and surface area of the stack based on Genetic Algorithm (GA) and thus obtained the maximum power density of the stack under working load. Peng et al.[13] applied support vector machines to the optimization of battery parameters. They proposed a GA for model structure identification, and the resulting model can be successfully generalized to different fuel cells and different operating conditions. Li et al.[14] combined GA and CFD to optimize the structural parameters of PEMFC with lumped flow channels, and considered the effects of output power and pressure drop. Hao et al.[15] used an artificial neural network approach combined with response surface analysis and NSGA-II algorithm to obtain the optimal configuration of a double inverted trapezoidal tapered channel structure and its associated dimensional parameters. In the research of proton exchange membrane fuel cells, data-driven machine learning methods play a crucial role in optimizing cell performance. Among them, support vector regression (SVR) and

[1]School of Undergraduate Education, Shenzhen Polytechnic University, Shenzhen 518055, China. [2]Shenzhen Institute of Advanced Research, University of Electronic Science and Technology of China, Shenzhen 518038, China. ✉email: liukunxiang19@mails.ucas.ac.cn; zhaochen913@163.com

Gaussian process regression (GPR) stand out, yet their performances vary depending on different conditions. When compared with commonly used regression models, linear regression struggles to handle the complex nonlinear relationships within fuel cells; polynomial regression can deal with certain nonlinearity, but it is prone to overfitting due to high-degree terms; neural network-based regression models are highly flexible but require a large amount of data and computing resources and lack interpretability. In contrast, SVR, based on the principle of structural risk minimization, has advantages when dealing with data following a normal distribution and in small sample sizes, and can maintain a certain level of interpretability. GPR, based on Bayesian theory, has excellent adaptability to various data distributions and can quantify uncertainties. Considering the complex nonlinearities, limited data availability, and the requirement for model interpretability in fuel cell research, SVR and GPR are reasonable choices for optimizing the cathode flow channel structure in this study due to their own advantages and complementary nature.

Recent research on air-cooled open cathode proton exchange membrane fuel cells (AO-PEMFC) has made breakthroughs in key areas. In terms of structural design, the annular flow channel and cathode channel bending design (e.g., optimized to a bending angle of 2.5°–5°) significantly improve the mass transfer efficiency and thermal management capability, and the annular structure improves the temperature uniformity by 3 times and increases the power by 15% while reducing the volume and weight. In the optimization of flow field topology, 3D wave channel, bionic flow field and vertical flow design promote the power density to increase by 8.5% by strengthening oxygen transfer and water discharge, but the high manufacturing complexity needs to be solved. In the process parameter study, the optimization of bolt preload, the synergistic application of "dual-stack configuration" and fan suction mode enhance the current density (1.12 V at 0.6 A/cm^2), while the fine tuning of anode channel depth and width further balances the gas pressure and humidity risk. At the level of environmental adaptability, research on high-temperature dehydration (95% power degradation at humidity < 10%), low-temperature freezing, and air pollutants provides a direction for improvement in extreme scenarios. Future trends focus on three major directions: intelligent algorithm-driven multi-objective optimization, durability breakthroughs in extreme conditions, and low-cost mass production processes for complex flow channels. In addition, such high-efficiency lightweight technology is particularly suitable for long endurance power for UAVs, high-efficiency integration of portable power supplies and reliable energy supply scenarios for automotive auxiliary systems, and shows a broad engineering prospect[16–22].

On the other hand, during the operation of AO-PEMFC, the cathode flow channel of the cell is the supply channel for the reactants and the discharge channel for the reaction-generated water and the reaction-generated heat, so its structure has a greater impact on the heat and mass transfer, hydrothermal management, the uniformity of the gas and current distributions and the electrochemical reactions inside the cell. A larger bending angle can disrupt the smooth flow of reactant gases, leading to local turbulence. This turbulence affects the gas distribution within the cell, increasing the mass transfer resistance in some regions. As a result, the availability of reactants for electrochemical reactions becomes uneven, reducing the overall electrochemical reaction rate. A wider channel allows for a greater flow cross-section, which can enhance the gas flow rate and improve the supply of reactants. However, if the width is too large, it may cause a decrease in the gas velocity in some areas, resulting in poor mixing of reactants and a negative impact on the uniformity of gas distribution. This, in turn, affects the heat and mass transfer processes and the efficiency of electrochemical reactions. An appropriate height can ensure a proper balance between gas flow and heat dissipation. A taller channel may increase the residence time of gases, which is beneficial for full-fledged electrochemical reactions. But an overly high channel may also lead to excessive heat accumulation due to slower heat dissipation, affecting the stability of the membrane-electrode assembly and ultimately reducing the cell performance. Zhao et al.[23] investigated the optimal channel size by adjusting the structural parameters of the cathode side channel, and experimentally investigated the effects of different cathode widths and channel angles on the battery performance, and found that different structural parameters of the cathode channel directly affect the contact resistance, cathode oxygen transport partial pressure, and ultimately have a significant impact on the output performance of the stack. Jang et al.[24] investigated the effect of cathode side channel openings on performance. The experimental results showed that single cells with larger openings of cathode side channels and slit-type open cathode channels have higher cell output performance. Thomas et al.[25] compared the air mass transfer synergies of different cathode-side channel widths, depths, and grooves, and found that the addition of grooves inside the channels directly affects the gas transport and temperature distribution, which ultimately affects the performance of the battery. Although these studies can find the optimal cathode channel structure parameters within the design range, they often fall into the local error range, and there are problems such as long cycle time and low efficiency.

In summary, the cathode channel structure of AO-PEMFC has a typical nonlinear, multiparameter, and strongly coupled relationship with the complex physical problems inside the cell. Performance prediction and optimization of cathode channel parameters based on experimental and numerical simulations have been widely used in scientific research and engineering practice of AO-PEMFC. On the other hand, data-driven machine learning methods tend to converge to a local optimum by gradient descent, which has obvious advantages in the study of optimization of channel structure parameters. The Kernel Based Extreme Learning Machine (KELM) has rarely been applied in the optimization modeling of cathode channel structure in AO-PEMFC. Therefore, this study will focus on the key scientific problem of simulation analysis and multi-objective optimization of AO-PEMFC channel modeling containing different cathode flow structures, so as to give the optimal parameters of cathode flow channels of fuel cells more efficiently and accurately. A three-dimensional, non-isothermal PEMFC simulation model was firstly developed by Computational Fluid Dynamics (CFD) method and the model accuracy was verified. The 360 sets of data obtained from the CFD simulations were then used as a dataset to input and train two agent models, Support Vector Regression (SVR) and Gaussian Process Regression (GPR). Finally, the agent models are optimized using GA to obtain the respective maximum power densities of the

models as well as the corresponding optimal channel parameters, which are further analyzed to give a range of engineering recommendations for the width, height, and bending angle of the channels.

Physical models and numerical methods

The physical model of the AO-PEMFC is shown in Fig. 1. It consists of identical serpentine anode channels (Fig. 1a), and cathode channels with different bending angles (Fig. 1b) Set the angle between the tangent direction of the bend avoidance at the entrance of the cathode channel and the horizontal direction as the bend angle, as shown in Fig. 1b. Between the cathode and anode flow channels is a Microelectrode Array (MEA), which specifically contains a gas diffusion layer (GDL), a catalytic layer (CL) and a PEM. The cathode and anode reactants enter the cathode and anode flow channel, and then uniformly diffuse through the GDL to the reaction surface of the CL to participate in the electrochemical reaction under the effect of pressure and concentration gradient. The water generated by the reaction is also discharged into the cathode channel and carried away by air under the effect of cathode and anode osmotic pressure. The cathode flow channel with different bending angles can further increase the velocity component perpendicular to the MEA, enhance the vertical diffusion of reactants, and improve the reaction efficiency. However, the bending angle varies along the direction of the channel, which may lead to uneven gas distribution in the channel and reduce the output performance. At the same time, the gas flow in the bent cathode channel also leads to certain turbulent kinetic energy and friction losses due to localized turns, which is not conducive to the reduction of parasitic loads. Therefore, there must exist a suitable range of cathode flow channel bending angles for AO-PEMFC to make the fuel cell output performance optimal. In this numerical study, the physical model of the fuel cell at four bending angles of 0°, 2.5°, 5° and 10° is established, and the parameters of other components in the model are consistent.

Optimization methods

There exists an intrinsic correlation between the different structural parameters of the bipolar plate, so the model optimized by the single-variable method adopted may not necessarily be the optimal model. Therefore, the multi-objective optimization algorithm is introduced into the development of fuel cell system performance model. In this study, the AO-PEMFC cathode channel structure was optimized, including the six-channel

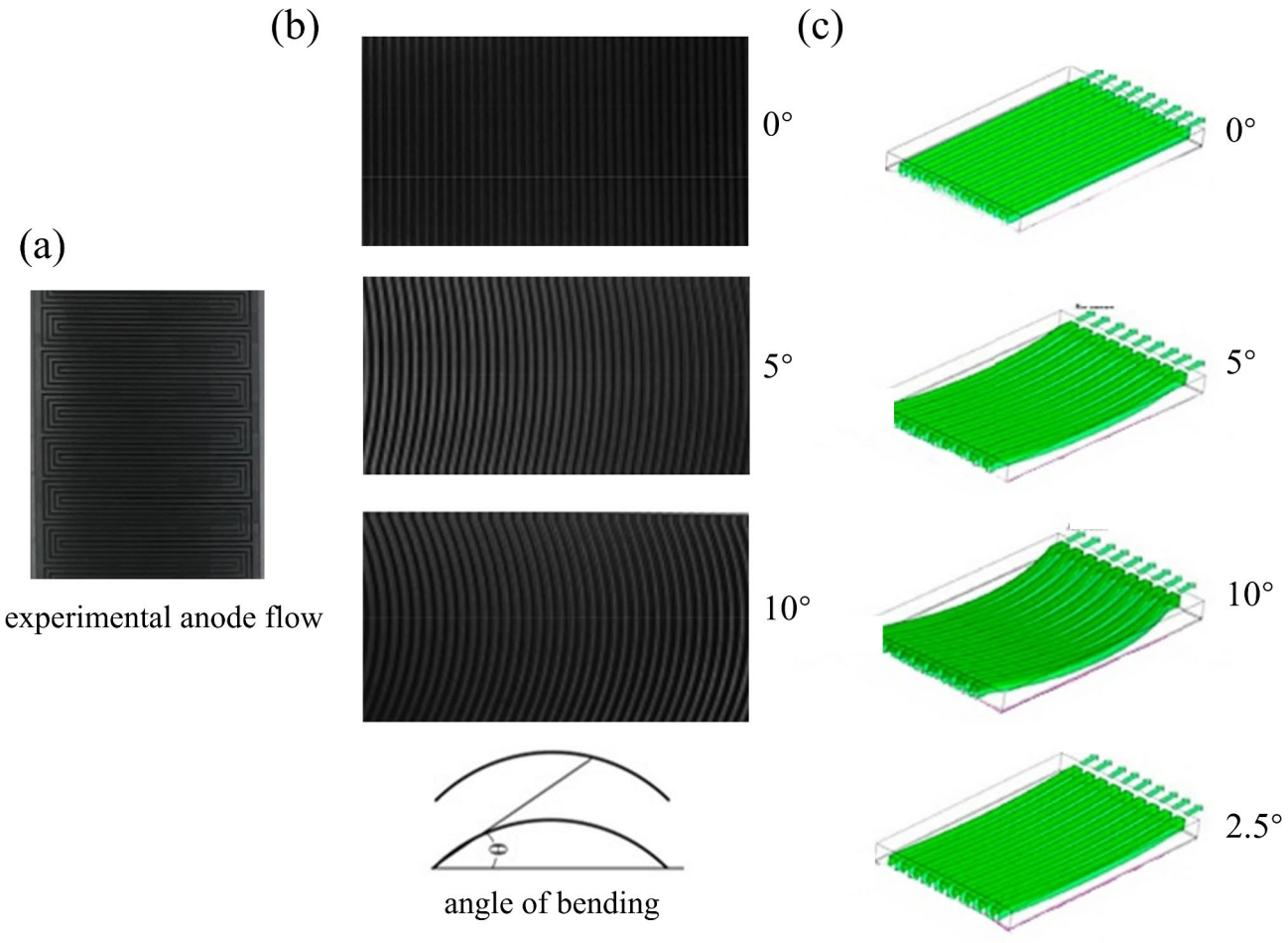

Fig. 1. (**a**) Anode plate design for experimental. (**b**) Different configurations of experimental cathode plate design. (**c**) Simulated configurations of AO-PEMFC for different cathode channel[18].

bending angle, single channel width and height. The optimization objective was higher output current density. Subsequently, multiple scale-free optimization of specific structural parameters was performed to obtain the best output performance.

Objective optimization methods and processes

In this study, we will choose to optimize the three parameters of cathode channel width (0.9–1.5 mm), depth (1.1–1.5 mm), and bending angle (0°-10°) on the geometrical parameters of the above single-cell numerical model and divide the data set according to the ratio of the training set to the test set of 7:3, as detailed in Table 1. By combining the full factorial design for the range of working conditions of the variables in the table, then the data set used for the agent model can be obtained through simulation, a total of 360 sets, in which the training set and test set are divided in the ratio of 7:3. GA optimization is also carried out with the main claim of improving fuel cell performance, i.e. maximum output power. Specifically, two proxy models, SVR and GPR, are constructed and trained to investigate the feasibility, advantages and disadvantages of both models when used to predict the power density of the battery in engineering practice. Then, the proxy models are used as fitness functions for GA optimization to obtain the maximum power density and the corresponding channel structure parameters of each of the two models, and are further analyzed to give the engineering recommendation ranges of the channel structure parameters.

Agent model

In this study, two agent models were constructed using SVR and GPR, respectively. Meanwhile, three different evaluation indexes are introduced to evaluate the prediction performance of the two proxy models in this paper. The three metrics are Mean Absolute Error (MAE), Root Mean Squared Error (RMSE) and Goodness of Fit R^2. The formulas for each of the three indicators are

$$MAE = \frac{1}{n}\sum_{i=1}^{n}|P_{i-}\prime P_i| \tag{1}$$

$$RMSE = \sqrt{\frac{1}{n}\sum_{i=1}^{n}(P_{i-}\prime P_i)^2} \tag{2}$$

$$R^2 = 1 - \frac{\sum_{i=1}^{n}(p_i\prime - P_i)^2}{\sum_{i=1}^{n}\left(p_i\prime - \overline{P_i}\right)^2} \tag{3}$$

where P_i is the power density value in the dataset; P_i' is the power density value predicted by the model; and $\overline{P_i}$ is the average of the power density values in the dataset.

SVR is an extension of Support Vector Machine (SVM). Similar to the traditional regression model, the model formula for linear SVR is as follows:

$$y = f(X) = \omega^T X + b \tag{4}$$

In the formula: y is a vector of predicted values of size $1 \times N$; X is an input matrix of size $D_{in} \times N$ with components of the form $[x_1, x_2, \ldots, x_N]$; ω is a vector of coefficients of size $D_{in} \times 1$; and b is a bias term. The model also has an explicit geometric meaning, which indicates that a spacing band of width 2εis constructed on both sides of the hyperplane centered on the hyperplane and all samples falling within this spacing band are considered to be predicted correctly, as shown in Fig. 2. In the SVR model of this paper, the interval band half-width ε is taken as 0.01.

GPR is a nonparametric probabilistic model that takes the Gaussian process as the prior, calculates the posterior distribution of the Gaussian process for new observations based on learning samples and certain assumptions, and outputs its mean as the predicted value.

Radial Basis Function (RBF) kernel is selected for the GPR model in this study and its expression is

$$\sigma f2\exp\left[-|x_i, x_j|^2 / \left(2l^2\right)\right]\sigma f2\exp\left[-|x_i, x_j|^2 / \left(2l^2\right)\right] \tag{5}$$

where σf^2 and l are the coefficient and length hyperparameters of the RBF kernel, respectively. The Marton kernel is a generalization of the RBF kernel with the expression

Input variable	Variable parameter values
Cathode channel width (mm)	0.5, 0.75, 1.0, 1.25, 1.5, 1.7
Cathode channel depth (mm)	0.5, 0.75, 1.0, 1.25, 1.5, 1.7
Cathode channel bending angle (°)	0, 2.5, 3, 4, 5, 6, 7, 8, 9, 10

Table 1. Parameter ranges for input variables.

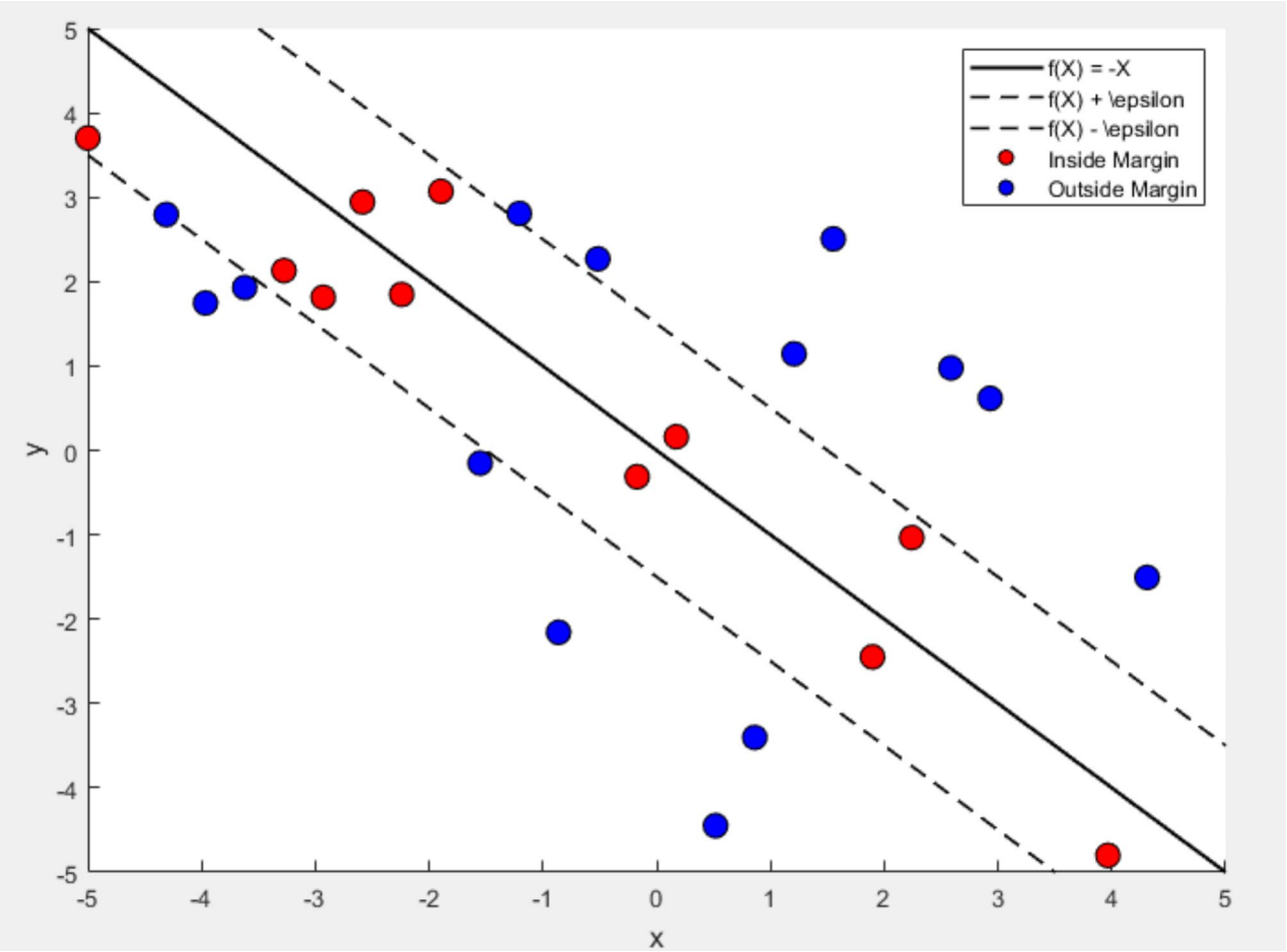

Fig. 2. Schematic of a one-dimensional linear SVR (samples within the error band are not counted as losses).

$$K_{Matern}(x_i, x_j) = \sigma f 2 \frac{2^{1-v}}{\Gamma(v)} \left(\frac{d\sqrt{2v}}{l} \right)^{v} K_v \left(\frac{d\sqrt{2v}}{l} \right), d = x_i - x_j \tag{6}$$

where Kv is the modified Bessel function and v is the smoothing degree parameter, which commonly takes the values of 1.5 and 2.5.

In this paper, we choose the Marton kernel with the smoothing degree parameter ν of 2.5 as the kernel function of the GPR model, and the hyperparameters σf^2 and l are set to 1.1^2 and 2.01, respectively.

Genetic algorithm optimization

GA is a population-based meta-heuristic algorithm, which simulates the genetic process of organisms in nature and the evolutionary process of natural selection, and contains three modules, namely, decoding encoding, individual fitness evaluation, and genetic operations, which generally include selection, crossover, and mutation, etc. The general flow of GA is shown in Fig. 3.

One bit of code represents a gene on a chromosome, one chromosome represents an individual organism, and all individuals make up a population, as shown in Fig. 4. The fitness function is used to evaluate the size of an individual's fitness, or how good the solution is; the larger the fitness, the better the individual, and the more the corresponding solution conforms to the optimal solution.

The purpose of GA is to identify the best individuals through the process of population evolution, which is achieved by genetic operations such as selection, crossover, and mutation. The selected best individuals can be directly inherited to the next generation, or pairwise crossover can produce new individuals and then be inherited to the next generation. The crossover and mutation operations are shown schematically in Fig. 5.

In this paper, we use the above two agent models as the fitness function, which is optimized by the GA to obtain the maximum output power of the fuel cell as well as the corresponding channel width, depth, and bending angle. In order to balance the solving efficiency and solving accuracy, the population size of GA is set to 20, and the maximum number of iterations of the population is 50. To strengthen the robustness of its genetic algorithm, the stochastic uniform operator is chosen. The specific parameters are detailed in Table 2.

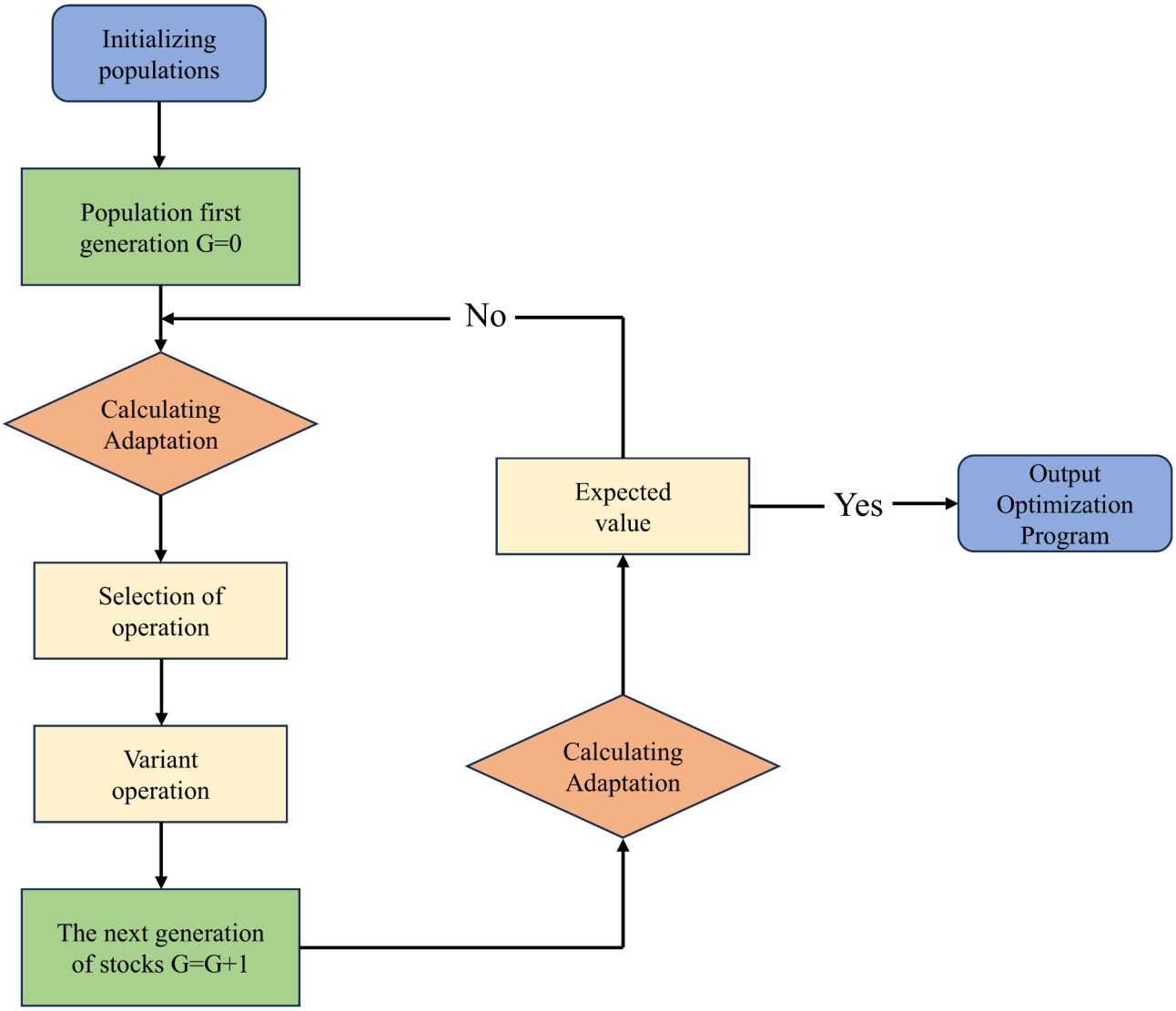

Fig. 3. Flowchart of the genetic algorithm.

Results and discussion

After training, the predicted values of the resulting model on the dataset are compared with the simulated values of the CFD. Figure 6 shows the correlation between the predicted and simulated values of the model on the training and test sets, respectively. The x-axis coordinates of the red dots in the figure represent the real values of the power density, i.e., the values calculated by the simulation of the CFD model; the y-axis coordinates represent the predicted values of the power density by the model; the blue solid line is a straight line with slope 1, and the closer the distribution of the red dots on both sides of the line, the better the prediction effect of the network.

It is evident from Table 3 that the true power density and the current density predicted by the two agent models have a better fit both in the training set and the test set. In particular, the model fit of GPR is slightly better than that of SVR, with R^2 of 0.99887 and 0.99988 in the test set and 0.99926 and 0.99958 in the training set, respectively. In addition, in terms of training time, GPR's training time is significantly shorter than SVR's under the same conditions, which is due to the fact that the GPR has fewer training parameters while the SVR spends most of its training time on hyperparameter search. SVR spends most of its training time on hyperparameter optimization, i.e., lattice search with cross-validation, which is one of the more time-consuming tasks in machine learning, and thus its training time is much longer than that of GPR.

Taking SVR as an example, Fig. 7 shows the variation of individual fitness of the population, where the best fitness corresponds to the best individual in the population, and the average fitness corresponds to the average value of fitness in the contemporary population. From Fig. 7, it can be clearly seen that after 50 computational iterations, the computational results converge, i.e., the average fitness value is equal to the best fitness value, indicating that the genetic algorithm optimization procedure has found the global optimal solution. The dashed line in Fig. 7 is obtained by fitting the scatter results. After continuous evolution, so that the final optimization

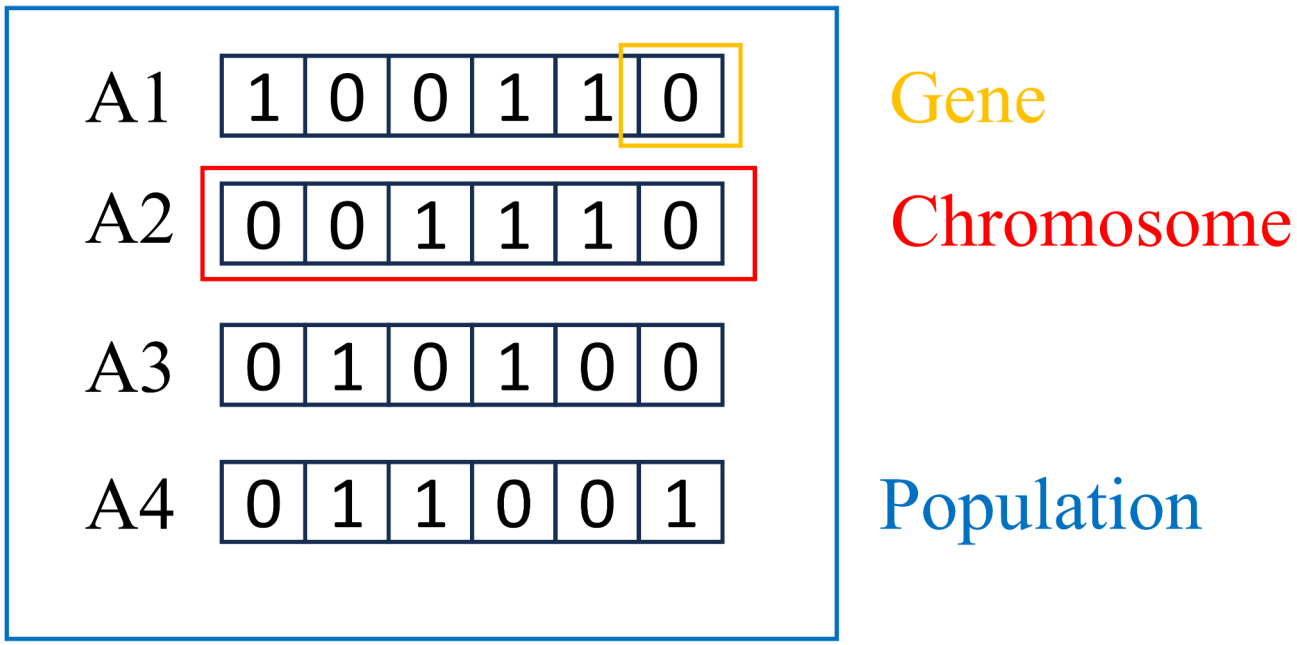

Fig. 4. Biological correspondence of codes.

result is basically unchanged because of the number of executions, at this time the optimization results obtained are shown in Table 4.

We had designed and fabricated single cells with different cathode channel widths (0.9–1.5 mm), and depths (1.1–1.5 mm) in previous studies to optimize the cell performance and temperature distributions under 2-mm-thick electrode plates in order to determine the ideal design parameters. It was concluded at that time that the optimal design parameters for the cathode channel were 1.1 mm as the optimal width at current densities less than 0.2 A/cm^2. Although 1.5 mm depth has the best performance, 1.3 mm depth is more suitable considering the strength of bipolar plate structure[23].

From the optimization results in Table 4, it can be seen that there are some differences in the optimization results of different models, but they are basically consistent with the CFD simulation results in the previous section, i.e., the maximum power density occurs in the bending angle results are near 2.5° and in the interval of the channel width of w = 1.05–1.2 mm, and in the interval of the channel height of d = 1.3–1.5 mm, and the maximum power density is 0.5012 W-cm^{-2} obtained. This is consistent with the results we have previously obtained through experimental testing.

It should be noted that the results in Table 4 cannot be directly used as suggested values in engineering practice for a number of reasons. In practice, due to the cost of actual fabrication and the different basic parameters of the bipolar plate for each model, and the fact that there will always be a certain deviation between the proxy model and the real value, i.e., the specific value of the optimization result is affected by certain random and subjective factors. However, although the specific values of the optimization results have a certain degree of variability, the range of variability can be regarded as limited, and there is no problem in using this range as a recommended range in the engineering practice of such fuel cells.

Implementing the optimized cathode channel structure in the actual manufacturing process presents both feasibility and challenges. In terms of manufacturing precision, although it is necessary to precisely control the channel width within the range of 1.05–1.2 mm, the height within 1.3–1.5 mm, and the bending angle within 2.23–2.99°, advanced manufacturing technologies currently available, such as micro-nano processing, are capable of meeting such precision requirements. Regarding cost, while high-precision manufacturing may lead to an increase in equipment and labor costs, these costs can be effectively controlled with the maturation of the process and large-scale production. When it comes to material selection, the materials need to possess good chemical stability, electrical conductivity, and thermal conductivity. Although common materials like graphite and metal alloys have their own advantages and disadvantages, new composite materials are currently under research and application, which are expected to balance performance and cost. In conclusion, when implementing the optimized cathode channel structure in practice, although it is necessary to comprehensively consider aspects such as manufacturing precision, cost, and material selection, these challenges are not insurmountable, and the overall difficulty is not overly high. The conclusions presented in this paper are feasible within the scope of engineering practice recommendations and can provide a reliable guiding basis for actual production.

Conclusions

The main conclusions obtained in this study include: extending the single-cell study variables as channel width, channel height and channel bending angle. The 360 sets of simulation results data obtained by full factorial design were also used as a dataset to input and train two proxy models, SVR and GPR. Finally, the agent models were

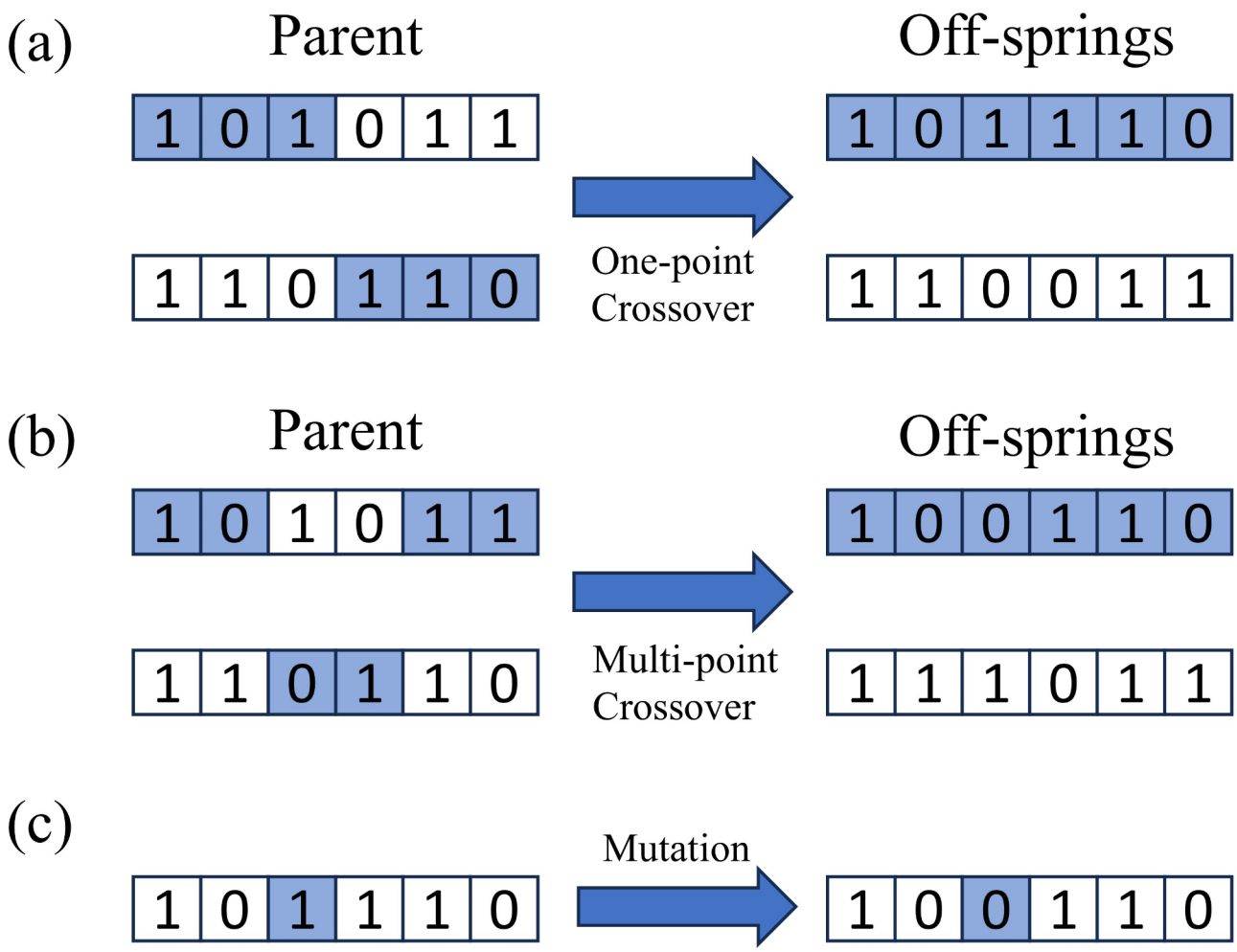

Fig. 5. Schematic representation of crossover and variation. (**a**) One-point crossover; (**b**) multi-point crossover; (**c**) mutation.

Model	Maximum power density
Population size	20
Number of iterations	50
Selection operator	Randomly distributed
Crossover probability	0.8
Probability of variation	0.005
Definition domain of fitness function	$w \in [0.9\ mm,\ 1.5\ mm]$, $d \in [1.1, 1.5\ mm]$, $\theta \in [0^\circ,\ 6^\circ]$ $\theta \in [0^\circ 10^\circ]$

Table 2. Genetic algorithm parameters.

optimized using a GA to obtain the models' respective maximum power densities and the corresponding optimal channel parameter ranges, which were w = 1.05–1.2 mm, d = 1.3–1.5 mm, and θ = 2.23–2.99°, respectively. The single-cell output power density in this range will be no less than 0.489W/cm^2.

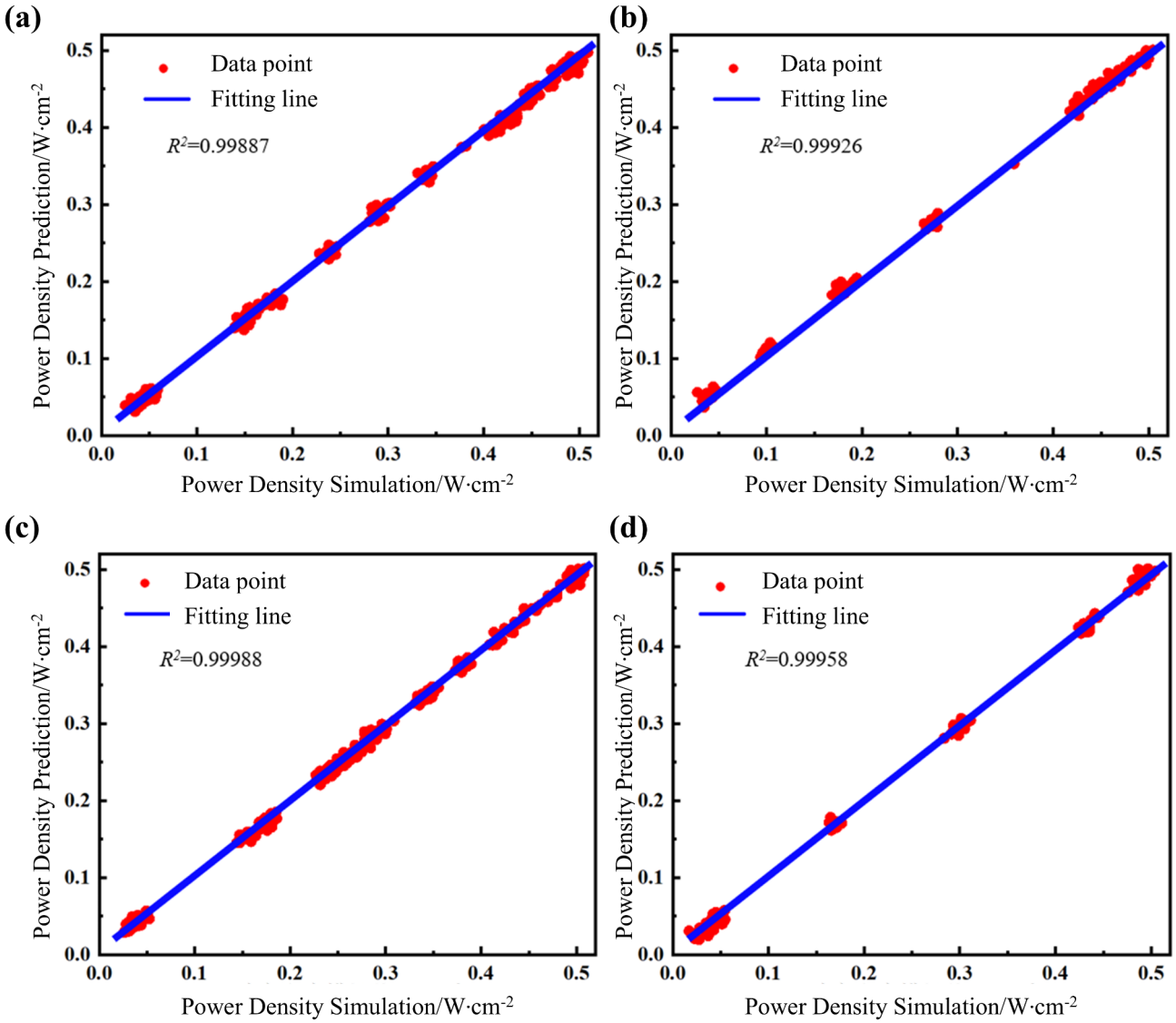

Fig. 6. SVR model predicted values versus CFD simulated values: (**a**) training set; (**b**) test set. GPR model predicted values versus CFD simulated values: (**c**) training set; (**d**) test set.

	Training set		Test set	
Evaluation metrics	**SVR**	**GPR**	**SVR**	**GPR**
MAE/W cm^{-2}	0.006859	0.001389	0.005963	0.003216
RMSE/W cm^{-2}	0.008654	0.003577	0.007856	0.00602
R^2	0.99887	0.99988	0.99926	0.99958

Table 3. Evaluation metrics for predictive performance of proxy models.

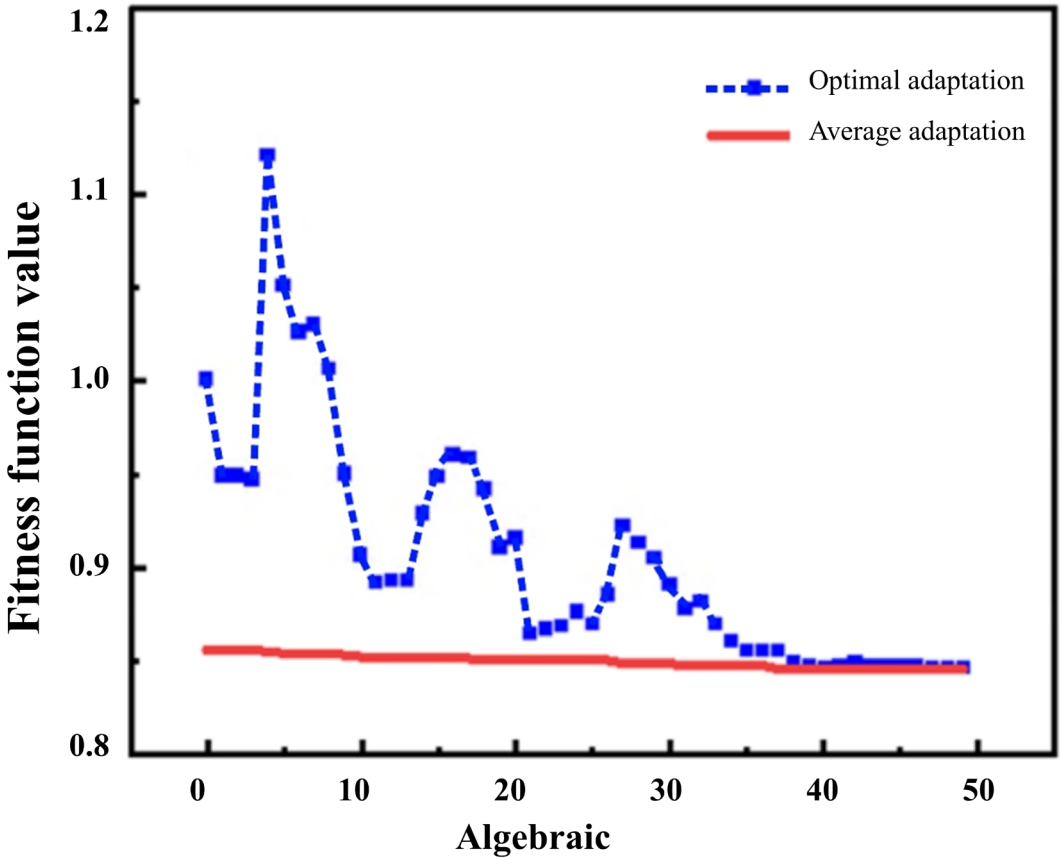

Fig. 7. Changes in individual fitness of populations.

Model	Maximum power density (P/W cm^{-2})	Channel width (w/mm)	Channel height (d/mm)	Channel bend angle (θ/°)
SVR	0.4998	1.0849	1.3254	2.2299
GPR	0.5012	1.1568	1.4685	2.9856

Table 4. Optimization results.

Data availability

Relevant data and modeling code in the article can be requested by contacting the corresponding author.

Received: 10 February 2025; Accepted: 8 April 2025
Published online: 03 May 2025

References

1. Jiao, K. et al. Designing the next generation of proton-exchange membrane fuel cells. *Nature* **595**, 361–369. https://doi.org/10.1038/s41586-021-03482-7 (2021).
2. Kovač, A., Paranos, M. & Marciuš, D. Hydrogen in energy transition: A review. *Int. J. Hydrogen Energy* **46**, 10016–10035. https://doi.org/10.1016/j.ijhydene.2020.11.256 (2021).
3. Olabi, A. G., Wilberforce, T. & Abdelkareem, M. A. Fuel cell application in the automotive industry and future perspective. *Energy* **214**, 118955. https://doi.org/10.1016/j.energy.2020.118955 (2021).
4. Sharaf, O. Z. & Orhan, M. F. An overview of fuel cell technology: Fundamentals and applications. *Renew. Sustain. Energy Rev.* **32**, 810–853. https://doi.org/10.1016/j.rser.2014.01.012 (2014).
5. Yin, P. et al. Machine-learning-accelerated design of high-performance platinum intermetallic nanoparticle fuel cell catalysts. *Nat. Commun.* **15**, 415. https://doi.org/10.1038/s41467-023-44674-1 (2024).
6. Echabarri, S., Do, P., Vu, H.-C. & Bornand, B. Machine learning and Bayesian optimization for performance prediction of proton-exchange membrane fuel cells. *Energy AI* **17**, 100380. https://doi.org/10.1016/j.egyai.2024.100380 (2024).
7. Yuan, H., Tan, D., Wei, X. & Dai, H. Fault diagnosis of fuel cells by a hybrid deep learning network fusing characteristic impedance. *IEEE Trans. Transport. Electr.* **10**, 1482–1493. https://doi.org/10.1109/tte.2023.3272654 (2024).
8. Zhang, Y. et al. Data-driven optimization of high-dimensional variables in proton exchange membrane water electrolysis membrane electrode assembly assisted by machine learning. *Ind. Eng. Chem. Res.* **63**, 1409–1421. https://doi.org/10.1021/acs.iecr.3c03546 (2024).

9. Kaiser, R. & Park, J.-C. Machine learning optimization of operating parameters to achieve high power density and efficiency of polymer electrolyte membrane fuel cell. *Chem. Eng. Sci.* **297**, 120309. https://doi.org/10.1016/j.ces.2024.120309 (2024).
10. Zhou, X. et al. Machine learning-assisted design of flow fields for proton exchange membrane fuel cells. *J. Power Sources* **626**, 235753. https://doi.org/10.1016/j.jpowsour.2024.235753 (2025).
11. Ghorbanzade Zaferani, S. P. et al. Prediction and optimization of sustainable fuel cells behavior using artificial intelligence algorithms. *Int. J. Hydrog. Energy* **52**, 746–766. https://doi.org/10.1016/j.ijhydene.2023.03.335 (2024).
12. Mohamed, I. & Jenkins, N. Proton exchange membrane (PEM) fuel cell stack configuration using genetic algorithms. *J. Power Sources* **131**, 142–146. https://doi.org/10.1016/j.jpowsour.2004.01.012 (2004).
13. Peng, X., Wu, W., Zhang, Y. & Yang, W. Determination of operating parameters for PEM fuel cell using support vector machines approach. *J. Energy Storage* **13**, 409–417. https://doi.org/10.1016/j.est.2017.09.005 (2017).
14. Li, W.-Z. et al. Optimization of blocked channel design for a proton exchange membrane fuel cell by coupled genetic algorithm and three-dimensional CFD modeling. *Int. J. Hydrogen Energy* **45**, 17759–17770. https://doi.org/10.1016/j.ijhydene.2020.04.166 (2020).
15. Hao, J. et al. Flow channel structure optimization and analysis of proton exchange membrane fuel cell based on the finite data mapping and multi-field synergy principle. *Int. J. Heat Mass Transf.* **207**, 123997. https://doi.org/10.1016/j.ijheatmasstransfer.2023.123997 (2023).
16. Zhang, J., Wang, C. & Zhang, A. Experimental study on temperature and performance of an open-cathode PEMFC stack under thermal radiation environment. *Appl. Energy* **311**, 118646. https://doi.org/10.1016/j.apenergy.2022.118646 (2022).
17. Deng, Z., Li, B., Xing, S., Zhao, C. & Wang, H. Experimental investigation on the anode flow field design for an air-cooled open-cathode proton exchange membrane fuel cell. *Membranes (Basel)* **12**, 1069. https://doi.org/10.3390/membranes12111069 (2022).
18. Zhang, L., Wu, X., Deng, Z. & Zhao, C. Performance improvement and numerical study on cathode channel for air-cooled open-cathode proton exchange membrane fuel cells. *Eng. Appl. Comput. Fluid Mech.* **18**, 2351958. https://doi.org/10.1080/19942060.2024.2351958 (2024).
19. Geng, Q., Han, Y., Li, B., Deng, Z. & Zhao, C. Testing study of different flow direction and structure for air-cooled proton exchange membrane fuel cell. *IEEE Access* **11**, 126172–126181. https://doi.org/10.1109/access.2023.3330181 (2023).
20. Zhao, R., Hu, M., Pan, R. & Cao, G. Disclosure of the internal transport phenomena in an air-cooled proton exchange membrane fuel cell—Part I: Model development and base case study. *Int. J. Hydrogen Energy* **45**, 23504–23518. https://doi.org/10.1016/j.ijhydene.2020.06.171 (2020).
21. Deng, Z., Liu, K., Xing, S. & Zhao, C. Optimization of cathode channel design, bolt torque, and assembly mode for enhanced performance in air-cooled proton exchange membrane fuel cells. *Int. J. Hydrogen Energy* **102**, 702–714. https://doi.org/10.1016/j.ijhydene.2025.01.119 (2025).
22. Zhao, C., Li, B., Zhang, L., Han, Y. & Wu, X. Novel optimal structure design and testing of air-cooled open-cathode proton exchange membrane fuel cell. *Renew. Energy* **215**, 118899. https://doi.org/10.1016/j.renene.2023.06.020 (2023).
23. Zhao, C., Xing, S., Chen, M., Liu, W. & Wang, H. Optimal design of cathode flow channel for air-cooled PEMFC with open cathode. *Int. J. Hydrogen Energy* **45**, 17771–17781. https://doi.org/10.1016/j.ijhydene.2020.04.165 (2020).
24. Jang, W. K., Choi, J., Seo, Y. H. & Kim, B. H. Effect of cathode flow field configuration on air-breathing proton exchange membrane fuel cell. *Int. J. Precis. Eng. Manuf.* **16**, 1129–1134. https://doi.org/10.1007/s12541-015-0146-6 (2015).
25. Thomas, S. et al. An experimental and simulation study of novel channel designs for open-cathode high-temperature polymer electrolyte membrane fuel cells. *Appl. Energy* **165**, 765–776. https://doi.org/10.1016/j.apenergy.2015.12.011 (2016).

Acknowledgements

This work was financially supported by Research Projects of Department of Education of Guangdong Province (2023ZDZ X3078), Guangdong Basic and Applied Basic Research Foundation (2024A1515012610).

Author contributions

Z.D. and K.L. wrote the main manuscript text. Q.W., X.F. and Y.H. prepared Figs. 1–7. C.Z. wrote and reviewed the manuscript.

Competing interests

The authors declare no competing interests.

Additional information

Correspondence and requests for materials should be addressed to K.L. or C.Z.

Reprints and permissions information is available at www.nature.com/reprints.

Publisher's note Springer Nature remains neutral with regard to jurisdictional claims in published maps and institutional affiliations.